

Extended MARTINI Water Model for Heat Transfer Studies

Sumith Yesudasan

Department of Mechanical Engineering, University of Jamestown, Jamestown, ND 58405, USA

Corresponding author email: sumith.yesudasan@uj.edu

Abstract

The computationally efficient classical MARTINI model is extended to simulate heat transfer simulations of water. The current MARTINI model, variations of it and other coarse grain water models focus on reproducing the thermodynamic properties below room temperature, hence making them unsuitable for studying high temperature simulations especially evaporation at 100°C. In this work, the MARTINI model is reparametrized using a linear search algorithm and conducting a series of simulations to match the phase equilibrium properties of water. The reparametrized model (MARTINI-E) accurately reproduces liquid density vs temperature and outperforms other leading coarse grain water models in enthalpy of vaporization and vapor density. This new water model can be used for simulating phase change phenomena and other energy transport mechanisms accurately.

Keywords: MARTINI, CGMD, water models, Molecular Dynamics, Optimization

Introduction

Evaporation of water is an important phenomenon to study in the area of heat transfer. In the semi-conductor industry and solar photovoltaics, the emergence of higher energy density calls for highly efficient and faster cooling systems. Water, which has a high specific heat capacity and high enthalpy of vaporization is a potential candidate for such systems. Based on kinetic theory [1], an evaporative heat flux of 20,000 W/cm² can be achieved using water. Thin film evaporation has a high potential to remove heat compared to bulk region [2, 3]. However, even with the recent developments in Nano-scale fabrication techniques the maximum heat flux is limited to 500 to 1000 W/cm²[4]. This points out to our poor understanding of the nanoscale evaporation of water. Studying water evaporation at nanoscale using experiments is a challenging attempt. Use of molecular dynamics can become helpful in this scenario[5-11], however there is no single water model which can capture or simulate all of its properties[12]. Even the best performing and widely used models are unsuitable to study evaporation, due to the computational cost.

This shifts our focus to computationally faster models called coarse grain molecular dynamics (CGMD) models. In a CGMD model, one or more water molecules are combined into a bead to represent the bulk properties of the system. Most of the existing CGMD models are developed for the use of biomolecular study[13, 14] and is not tested for heat transfer. The existing models mainly focus on the room temperature behavior of water or even sometimes the behavior below zero degree Celsius. While these models can capture freezing, ice formation and other properties of water, their applicability to high temperature applications is limited or seldom.

In this work, we present an extension to the existing model called MARTINI[15], which represents four water molecules as a single bead. A simple search algorithm along with a fitness score function is used to parameterize the model. This model is computationally highly efficient and the extended model could reproduce many important thermodynamic properties of water at high temperatures. For the first time in literature, our CGMD model captures the density of water at temperature near 100°C. Also, it predicts the liquid-vapor co-existing system accurately and

enthalpy of vaporization of water in a range of temperatures from 350 K to 410 K.

Coarse Grain Models of Water

Though there exists a wide range of coarse grain water models, the present work focuses only on the models with a single bead. Among them, the classical MARTINI water model [15, 16], mW model [17], and the recently developed ML-mW model [18] can simulate most of the thermodynamic properties at temperatures near and below 300 K. However, their feasibility near temperatures of 373 K is not tested.

The MARTINI model maps a cluster of four water molecules to a single bead (Figure 1a) and interacts with each other using a standard Lennard Jones (LJ) potential (eq. 1).

$$E_{MARTINI} = 4\epsilon_{MARTINI} \left[\left(\frac{\sigma}{r} \right)^{12} - \left(\frac{\sigma}{r} \right)^6 \right] \quad (1)$$

Here, for water $\epsilon_{MARTINI} = 5 \text{ kJ/mol} = 1.19503 \text{ kcal/mol}$ and $\sigma = 0.47 \text{ nm}$ are standard parameters. In the computer simulations this LJ interaction potential is shifted (both potential and force smoothly goes to zero) and a cutoff distance $r_{cut} = 1.2 \text{ nm}$, corresponding to approximately 2.5σ is used. These parameters and potential function corresponds to MARTINI 2.0 [16].

While MARTINI models are simple in construction, they need additional anti-freeze particles to keep water from freezing above 273 K. In this context, other models like mW [17] and

ML-mW [18] uses Stillinger-Weber (SW) potential [19] which enables more accurate representation of water. In these models, one water molecule is mapped onto one coarse grain bead as shown in the Figure 1a. The functional form of SW potential is as shown in below equations.

$$E = \sum_i \sum_{j>i} \phi_2(r_{ij}) + \sum_i \sum_{j \neq i} \sum_{k>j} \phi_3(r_{ij}, r_{ik}, \theta_{ijk}) \quad (2)$$

$$\phi_2(r_{ij}) = A_{ij} \epsilon_{ij} \left[B_{ij} \left(\frac{\sigma_{ij}}{r_{ij}} \right)^{p_{ij}} - \left(\frac{\sigma_{ij}}{r_{ij}} \right)^{q_{ij}} \right] \exp \left(\frac{\sigma_{ij}}{r_{ij} - a_{ij} \sigma_{ij}} \right) \quad (3)$$

$$\phi_3(r_{ij}, r_{ik}, \theta_{ijk}) = \lambda_{ijk} \epsilon_{ijk} \left[\cos \theta_{ijk} - \cos \theta_{0ijk} \right]^2 \exp \left(\frac{\gamma_{ij} \sigma_{ij}}{r_{ij} - a_{ij} \sigma_{ij}} \right) \exp \left(\frac{\gamma_{ik} \sigma_{ik}}{r_{ik} - a_{ik} \sigma_{ik}} \right) \quad (4)$$

The mW model of water used the SW potential and modeled water as an intermediate element between carbon and silicon. The parameters of this model are further improvised recently using machine learning algorithms. The description of the variables of SW potential and the parameters for mW and ML-mW are described elsewhere in literature [17-19]. Even though mW and ML-mW can simulate thermodynamic properties of water better than MARTINI model, the computational cost is high due to the smaller number of water molecule mapping per bead and also the presence of three body potential functions.

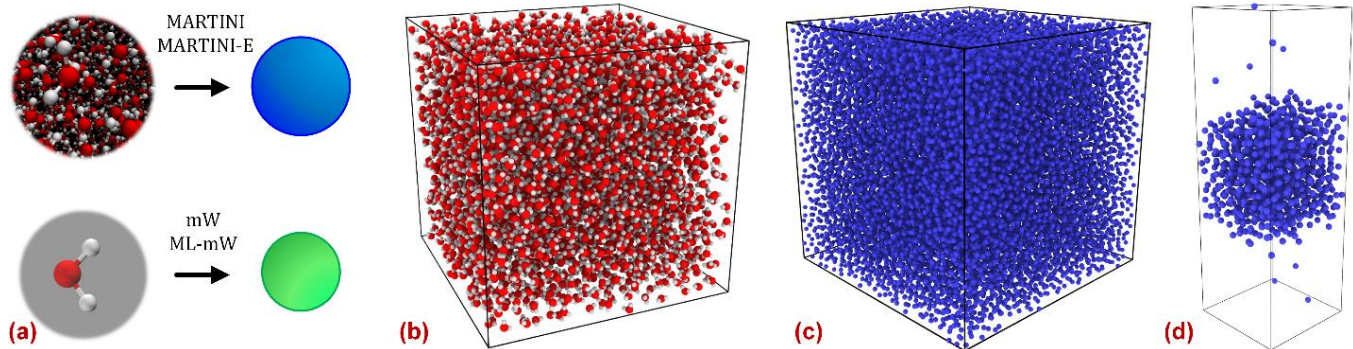


Figure 1: Coarse grain models of water. (a) four water molecules to form a single MARTINI and MARTINI-E bead, one water molecule to form a mW and ML-mW bead. (b) 5 nm cubic box of SPC/E water. (c) 20,000 MARTINI-E beads at a density corresponding to 372.76 K. (d) 1045 MARTINI-E beads in a vapor-liquid-vapor system.

The main objective of this paper is to extend the computationally efficient MARTINI model to simulate heat transfer near 100 °C. To achieve this the ϵ and σ parameters of MARTINI model is reparametrized to obtain accurate density, enthalpy of vaporization and self-diffusion coefficient over a range of temperatures. The final model (MARTINI-E) after parametrization is tested with a vapor-liquid-vapor system to check the variation of density and pressure profile. The coarse grain systems used for this study is shown in the Figure 1c and 1d. A 5 nm cube box of SPCE [20] water molecules are shown in Figure 1b for reference.

Coarse Graining Protocol

The coarse graining protocol used in this work is shown in the Figure 2. Initial parameters of the model are taken the same as original MARTINI model[16]. With this set, coarse grain molecular dynamics (CGMD) simulations are performed with a 20,000 bead system (large enough to avoid box size effect, if any) as shown in Figure 1c for a range of temperatures 350 K, 360 K, 370 K, 372.76 K, 375 K, 380 K, 390 K, 400 K, 410 K. These are the range of temperatures typically water based evaporative cooling systems are subjected to. The simulations are performed at saturated pressures corresponding to the temperature of the system. All simulations are performed using LAMMPS software [21] using a Nose-Hoover thermostat and barostat [22-24] with a chain length of four. From the simulations,

density of the system is estimated and compared to the experimental values from the NIST standard web book [25]. This comparison is made using a fitness score as described in the below equation.

$$Fitness\ score = \frac{100}{N_T} \sum_{i=1}^{N_T} \frac{\rho_{CGMD}^i}{\rho_{EXP}} \quad (5)$$

A fitness score closer to 100 means a very good agreement between the model and the experiments. If the score is not close enough to 100, then a scale is obtained by taking the inverse of the score multiplied by 100. Using this scale, the current parameters are scaled and the CGMD simulations are performed again. This process is continued until the difference between the fitness score and 100 becomes less than tolerance (0.1 %) as shown in the flow chart.

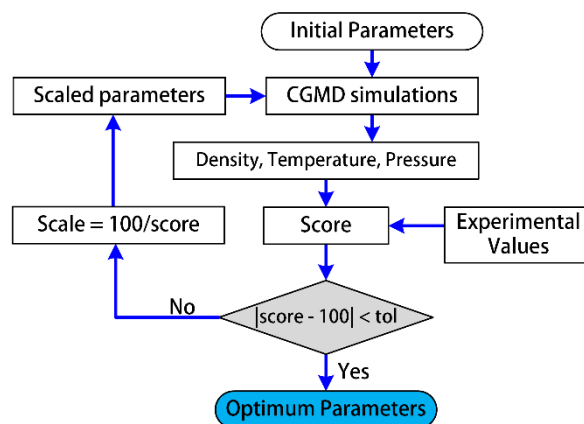


Figure 2: Protocol for searching the optimum MARTINI parameters using CGMD simulations

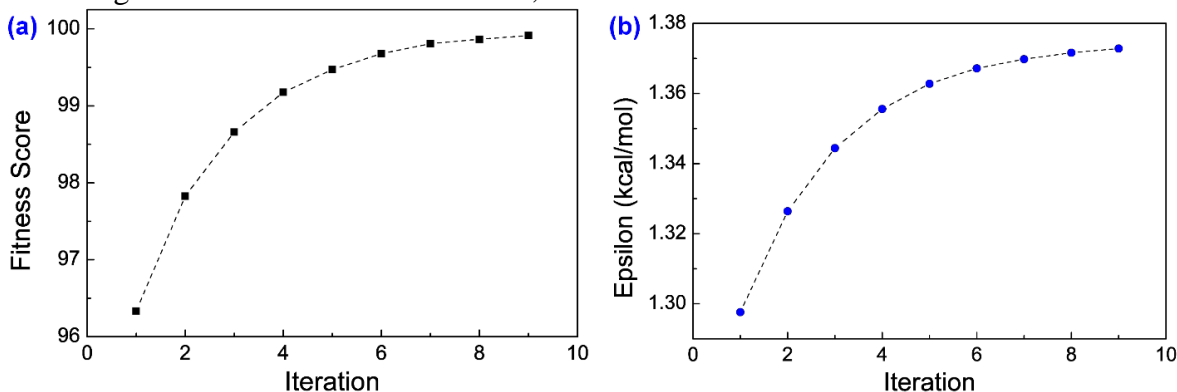


Figure 3: Parameter searching for MARTINI model. (a) Fitness score variation after each iteration. A score of 100 is perfect match with experimental results. (b) Arriving at the optimum value for the MARTINI epsilon parameter through every iteration.

Using the optimization protocol, after first iteration, the fitness score was 96.33 and ϵ was 1.297594 *kcal/mol*. After 9 iterations, the fitness score became 99.913 and ϵ became 1.371638229 *kcal/mol*. The model corresponding to this optimum parameter, we call as extended MARTINI model (MARTINI-E). The variation of fitness score and epsilon (energy parameter) with respect to the iterations are shown in the Figure 3.

The time step of integration used in a typical MARTINI model is 20 fs to 40 fs, but in optimization stage, we have used a time step of 5 fs. The CGMD simulations are run for 100,000 steps of equilibration and 200,000 steps of production run. The final parameters of the optimized water model are found to be $\epsilon_{MARTINI-E} = 1.371638229$ *kcal/mol* and $\sigma = 0.47$ nm.

Results

After the parametrization of the model, the next step is comparing its performance with original MARTINI model, mW and ML-mW models. For this purpose, a cubic box system with box length of 13.4σ (6.3 nm) with 2000 beads (corresponds to 8000 water molecules) are used for MARTINI and MARTINI-E models. Also, a 5 nm cubic box system with 4005 water molecules are used for mW and ML-mW models. By varying the temperature, density, self-diffusion coefficient and enthalpy of vaporization is estimated. For enthalpy of vaporization, a vapor system is considered with same number density, but appropriate vapor density by varying the system size.

The results of density variation are shown in the Figure 4a. The legends MAR, MAR-E, mW, ML-mW and EXP corresponds to original MARTINI, MARTINI-E, mW, ML-mW and Experimental values respectively. The density results show excellent match of MARTINI-E with experimental results. This is not surprising since the parametrization the model was done based on density matching.

The self-diffusion coefficient of the water from the CGMD simulations [26] are estimated by the following equation and shown in the Figure 4b.

$$D = \frac{1}{6} \lim_{t \rightarrow \infty} \frac{\langle [\vec{r}(t_0+t) - \vec{r}(t_0)]^2 \rangle}{t} \quad (6)$$

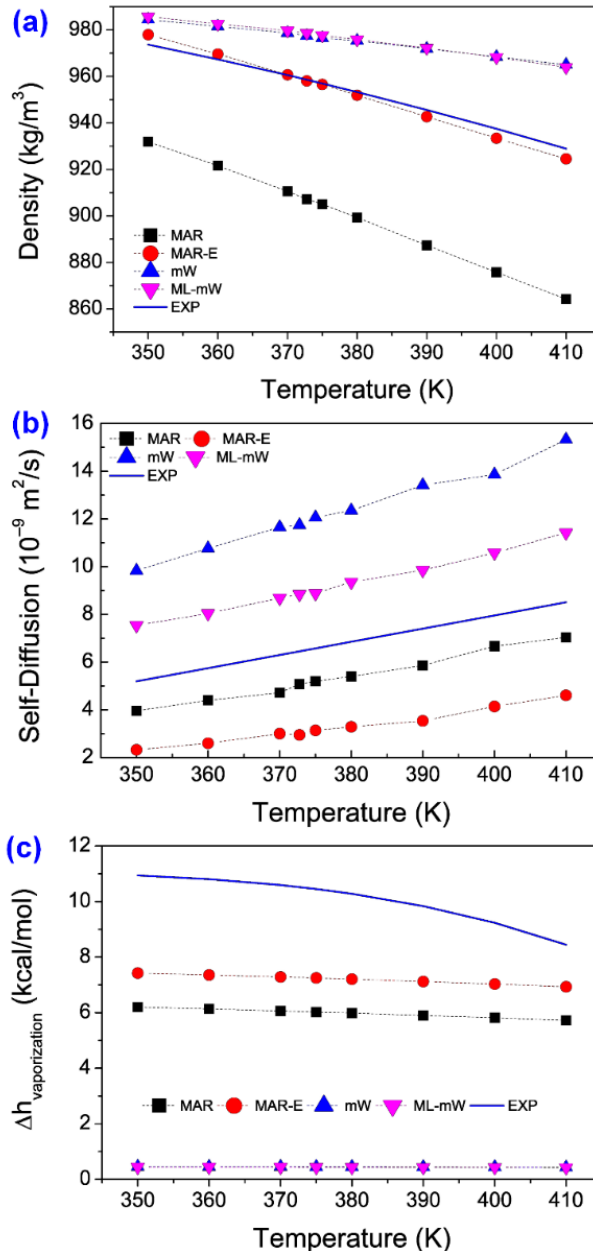


Figure 4: Variation of (a) density, (b) self-diffusion coefficient and (c) enthalpy of vaporization of various coarse grain water models with respect to temperature ranging from 350 K to 410 K.

The original MARTINI model and ML-mW models simulate self-diffusion coefficients of

water closer to experiments while MARTINI-E and mW models under perform. This is due to increasing potential strength (epsilon of LJ potential) inversely relates to the diffusion coefficient. This is case with mW potential too, the ϵ , A and B parameters of mW model is lower than ML-mW model making it more diffusible. The molecular models are visualized using VMD software [27] and OVITO software [28].

The enthalpy of vaporization is estimated from the simulations and plotted the variation with temperature in Figure 4c. At this temperature range, the mW and ML-mW performs poorly and MARTINI-E turns out to be the best among all. The MARTINI-E follows the same trend as MARTINI, but closer towards the experimental values. For heat transfer and evaporative studies of water, pressure, temperature, density and enthalpy of evaporation are the major factors of interest. MARTINI-E model performs well in predicting these variables, in and around the

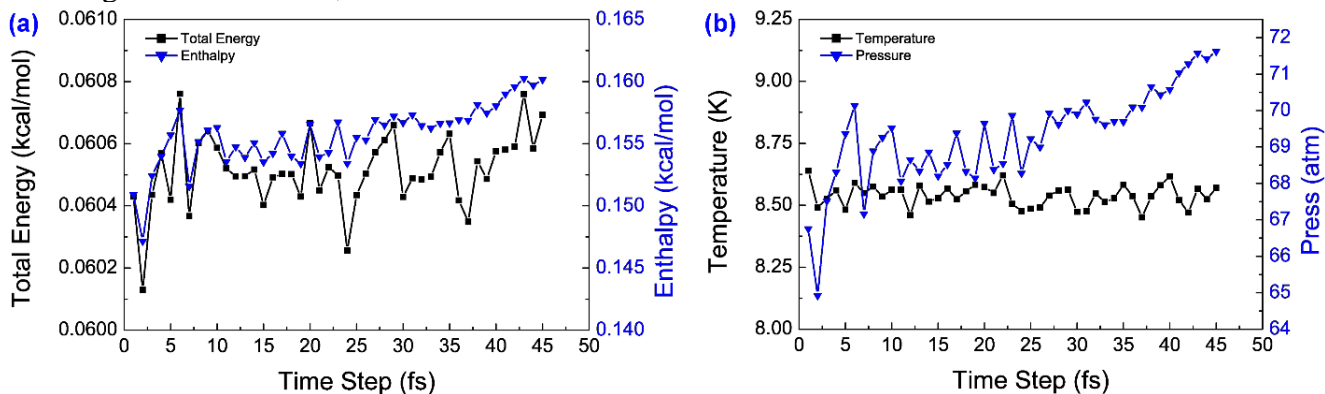


Figure 5: Fluctuation of Standard deviation of (a) total energy, enthalpy and (b) temperature and pressure with respect to time step of integration.

Simulating Liquid-Vapor coexisting system

Most of the heat transfer systems involving phase change process needs a model which can predict two phase co-existing properties correctly[8]. To investigate this, a vapor-liquid-vapor (VLV) lamellar like system (Figure 1d) is simulated with our MARTINI-E model and other CGMD models. A box size of $5\text{ nm} \times 5\text{ nm} \times 15\text{ nm}$ is used with 1045 beads forming liquid film in the middle is used for both MARTINI and MARTINI-E models. The same box size with

372.76 K (99.61°C, corresponds to standard boiling point).

Sensitivity of the timestep

The timestep for MARTINI models in the literature is suggested to be in the range of 20 fs to 30 fs [29, 30]. Here, we did a sensitivity study for the time step of integration for the MARTINI-E model. The fluctuations of the thermodynamic quantities like total energy, enthalpy, temperature, pressure is estimated in terms of standard deviation. For this purpose, the liquid system model with 2000 beads is subjected to 410 K (higher temperature will lead to higher fluctuations) under a Nose Hoover thermostat. This time the barostat is turned off. The variation of these quantities is given in the Figure 5. Our results show that these quantities fluctuate more after the time step of 25 fs. Hence a time step of 25 fs or below is recommended for the heat transfer simulations with MARTINI-E model.

4005 molecules are used for mW and ML-mW models. The number of beads and molecules are selected in a way that the liquid film thickness in the middle will be same in all cases and can make a comparison of system properties irrespective of the model type.

These CGMD systems are equilibrated for 100,000 steps and production run for 200,000 steps. A time step of integration of 1 fs is used for mW and ML-mW models, and 5 fs is used for MARTINI and MARTINI-E models. The Nose-

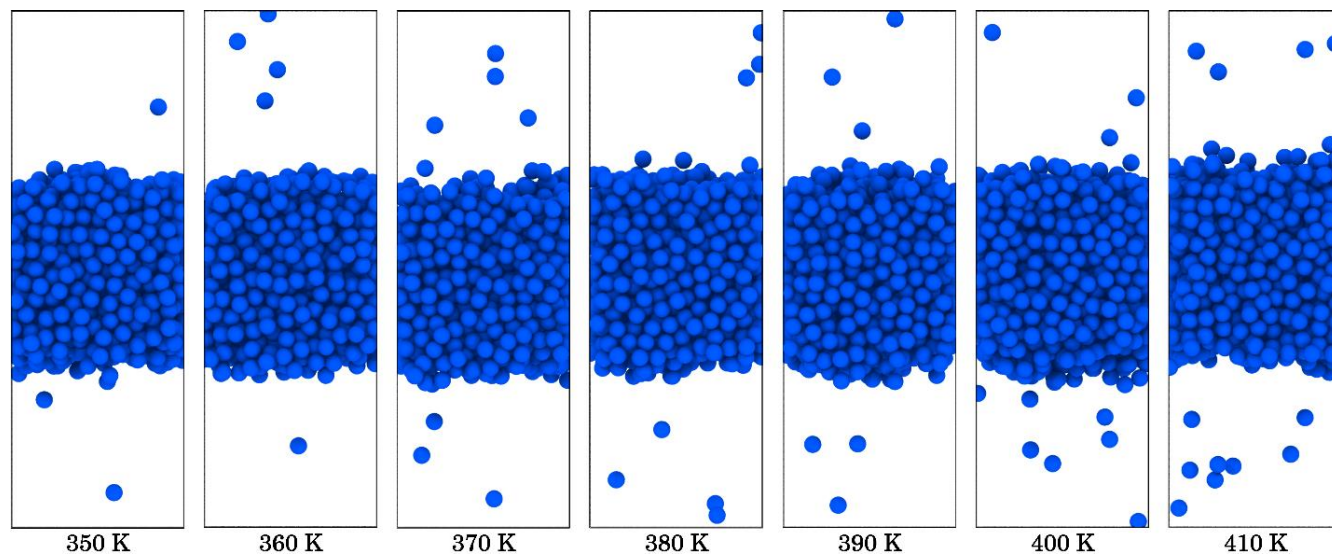


Figure 6: Snapshots of vapor-liquid-vapor system of MARTINI-E model at different temperatures.

Hoover thermostat is used to control the temperature and pressure is not controlled. The screenshots of resulting equilibrated system of

MARTINI-E model is shown in Figure 6 for various temperatures.

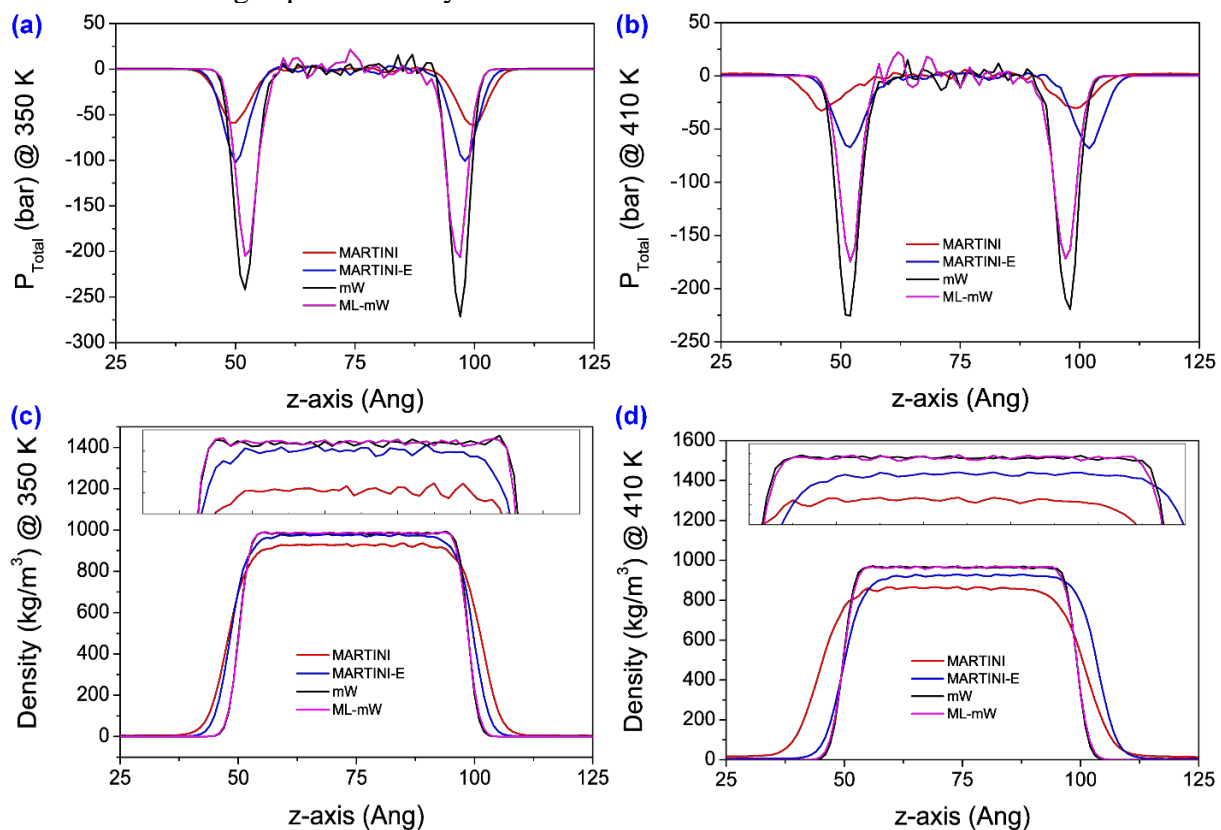


Figure 7: Total pressure profile of the vapor-liquid-vapor system at (a) 350 K and (b) 410 K. Density profile of the vapor-liquid-vapor system at (c) 350 K and (d) 410 K. The inset figures show a close-up of the fluctuations near liquid region. (color online)

To further understand the behavior of the system, the pressure and density profile along the length of the VLV system is time averaged to local bins and plotted in Figure 7. A triangular shape

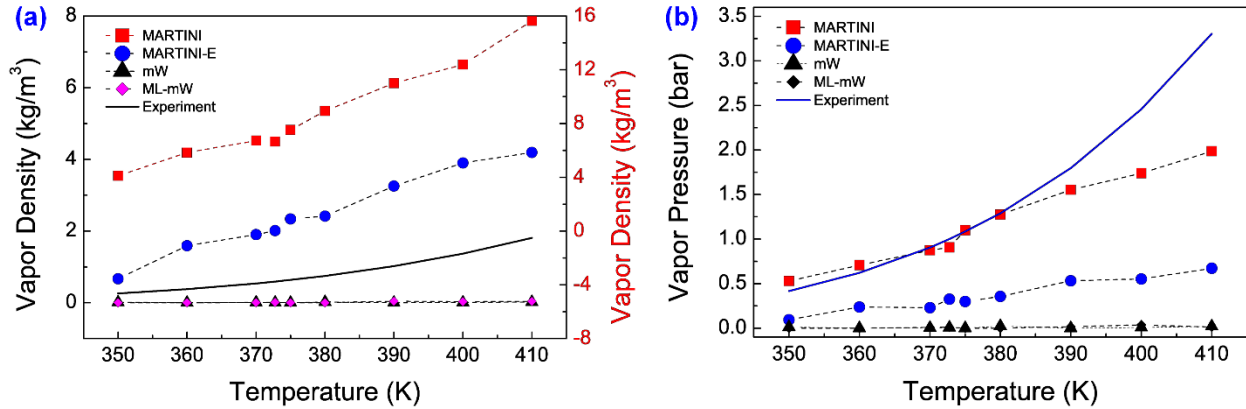


Figure 8: Temperature dependency of (a) vapor density and (b) vapor pressure of various CGMD models.

The resulting system shows a higher interfacial pressure for mW type models in comparison with MARTINI models. The results are shown for the lowest temperature (350 K) and highest temperature (410 K) used for the simulations. The pressure profiles show a high fluctuation for mW and ML-mW models near to the central region which are not significant in MARTINI and MARTINI-E models. The density profile shows a square like behavior for mW and ML-mW models which indicates a sharp liquid-vapor interface which is not realistic. At the same time both MARTINI models shown a smooth liquid-vapor interface which is realistic. A close-up view of the density profile near the liquid regions are shown in the inset of the Figure 7c,d.

There are no experimental pressure and density profiles of VLV water system to compare with, hence average quantities in the liquid and vapor regions are used for validation. The vapor quantities are estimated by averaging properties from bins 1 to 30 and 120 to 150 and liquid quantities are estimated by averaging from 60 to 90 bins.

The vapor density results (Figure 8a) shows that the MARTINI-E is closer to predict the experimental values. While mW and ML-mW appears to be closer to experimental curve, they

interpolation function [31] is used for the smooth distribution of pressure and density into the local bins.

are due to the absence of vapor molecules. In fact, mW and ML-mW models are poor models for predicting liquid-vapor interfacial properties. This is again reflected in the vapor pressure estimation as shown in the Figure 8b. But this time, the original MARTINI model shows better agreement with experiment than MARTINI-E.

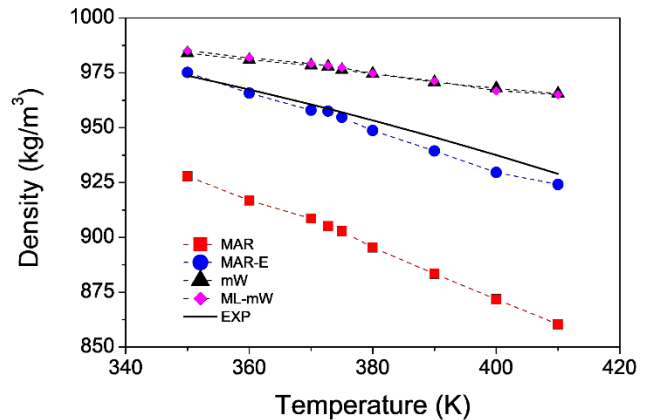


Figure 9: Density of liquid water in the middle of the film of a VLV system.

The analysis of the density in the liquid region Figure 9 shows a very good agreement with the experiments for the MARTINI-E model, while mW and ML-mW models over predict the density and original MARTINI model under predicts it. This is due to the lower epsilon value of MARTINI model and presence of 3 body

potential and short cutoff range for mW and ML-mW models.

Discussion

A simple extension of the MARTINI model by fixing the sigma of LJ potential and changing the epsilon has enabled to simulate a range of variables related to water at temperatures near 100°C. The new model (MARTINI-E) can accurately capture a variety of thermodynamic properties like vapor and liquid density at saturated temperature, enthalpy of vaporization etc. However, the use of overly simplistic LJ potential limits the ability to match a greater number of parameters. This calls for use of potential functions which can be tuned using a number of variables. Though the current study doesn't focus on dielectric properties, dipole moments, radial distribution function [32], etc. it may be beneficial for matching them for a more accurate version of the CGMD model.

References

- [1] W. Gambill, J. Lienhard, An upper bound for the critical boiling heat flux, *ASME J. Heat Transfer*, 111 (1989) 815-818.
- [2] S. Bigham, A. Fazeli, S. Moghaddam, Physics of microstructures enhancement of thin film evaporation heat transfer in microchannels flow boiling, *Scientific reports*, 7 (2017) 44745.
- [3] Q. Wang, R. Chen, Ultrahigh flux thin film boiling heat transfer through nanoporous membranes, *Nano letters*, 18 (2018) 3096-3103.
- [4] A. Jaikumar, A. Rishi, A. Gupta, S.G. Kandlikar, Microscale morphology effects of copper-graphene oxide coatings on pool boiling characteristics, *Journal of Heat Transfer*, 139 (2017) 111509.
- [5] S. Yesudasan, S. Chacko, Fast Local Pressure Estimation for Two Dimensional Systems From Molecular Dynamics Simulations, in: *ASME 2018 Power Conference collocated with the ASME 2018 12th International Conference on Energy Sustainability and the ASME 2018 Nuclear Forum*, American Society of Mechanical Engineers, 2018, pp. V002T010A004-V002T010A004.
- [6] Y. Sumith, S.C. Maroo, A direct two-dimensional pressure formulation in molecular dynamics, *Journal of Molecular Graphics and Modelling*, 79 (2018) 230-234.
- [7] S.Y. Daisy, S.C. Maroo, A robust algorithm for contact angle and interface detection of water and argon droplets, *Heat Transfer Engineering*, 38 (2017) 1343-1353.
- [8] S. Yesudasan Daisy, Molecular dynamics study of solid-liquid heat transfer and passive liquid flow, (2016).
- [9] S.C. Maroo, Surface-heating algorithm for water at nanoscale, *The journal of physical chemistry letters*, 6 (2015) 3765-3769.
- [10] Y. Akkus, A. Beskok, Molecular diffusion replaces capillary pumping in phase-change-driven nanopumps, *Microfluidics and Nanofluidics*, 23 (2019) 14.
- [11] Y. Akkus, A. Koklu, A. Beskok, Atomic Scale Interfacial Transport at an Extended Evaporating Meniscus, *Langmuir*, (2019).
- [12] W.L. Jorgensen, J. Chandrasekhar, J.D. Madura, R.W. Impey, M.L. Klein, Comparison of simple potential functions for simulating liquid water,

Conclusion

The classical MARTINI model is successfully extended to a higher temperature range which will enable it to use for heat transfer simulations. The extended model called as MARTINI-E is validated against a number of thermodynamic parameters including the co-existing points of temperature-pressure-density phase equilibrium. The new model is computationally faster like classical MARTINI model and at the same time can simulate liquid-vapor co-existence. The bulk liquid simulation and vapor-liquid-vapor system simulation using the new model and the existing CGMD models shows that the MARTINI-E outperforms them in simulating vapor density, liquid film density, and enthalpy of vaporization. These are critical parameters for simulating the water for heat transfer studies.

- The Journal of chemical physics, 79 (1983) 926-935.
- [13] S. Yesudasan, X. Wang, R.D. Averett, Fibrin polymerization simulation using a reactive dissipative particle dynamics method, *Biomechanics and Modeling in Mechanobiology*, 17 (2018) 1389-1403.
- [14] S. Yesudasan, X. Wang, R.D. Averett, Coarse-grained molecular dynamics simulations of fibrin polymerization: effects of thrombin concentration on fibrin clot structure, *Journal of molecular modeling*, 24 (2018) 109.
- [15] S.J. Marrink, A.H. De Vries, A.E. Mark, Coarse grained model for semiquantitative lipid simulations, *The Journal of Physical Chemistry B*, 108 (2004) 750-760.
- [16] S.J. Marrink, H.J. Risselada, S. Yefimov, D.P. Tieleman, A.H. De Vries, The MARTINI force field: coarse grained model for biomolecular simulations, *The journal of physical chemistry B*, 111 (2007) 7812-7824.
- [17] V. Molinero, E.B. Moore, Water modeled as an intermediate element between carbon and silicon, *The Journal of Physical Chemistry B*, 113 (2008) 4008-4016.
- [18] H. Chan, M.J. Cherukara, B. Narayanan, T.D. Loeffler, C. Benmore, S.K. Gray, S.K. Sankaranarayanan, Machine learning coarse grained models for water, *Nature communications*, 10 (2019) 379.
- [19] F.H. Stillinger, T.A. Weber, Computer simulation of local order in condensed phases of silicon, *Physical review B*, 31 (1985) 5262.
- [20] H. Berendsen, J. Grigera, T. Straatsma, The missing term in effective pair potentials, *Journal of Physical Chemistry*, 91 (1987) 6269-6271.
- [21] S. Plimpton, Fast parallel algorithms for short-range molecular dynamics, *Journal of computational physics*, 117 (1995) 1-19.
- [22] G.J. Martyna, M.E. Tuckerman, D.J. Tobias, M.L. Klein, Explicit reversible integrators for extended systems dynamics, *Molecular Physics*, 87 (1996) 1117-1157.
- [23] G.J. Martyna, D.J. Tobias, M.L. Klein, Constant pressure molecular dynamics algorithms, *The Journal of Chemical Physics*, 101 (1994) 4177-4189.
- [24] W. Shinoda, M. Shiga, M. Mikami, Rapid estimation of elastic constants by molecular dynamics simulation under constant stress, *Physical Review B*, 69 (2004) 134103.
- [25] E. Lemmon, Thermophysical properties of fluid systems, NIST Chemistry WebBook, (1998).
- [26] D. Keffer, The working man's guide to obtaining self diffusion coefficients from molecular dynamics simulations, Department of Chemical Engineering, University of Tennessee, Knoxville, (2001).
- [27] W. Humphrey, A. Dalke, K. Schulten, VMD: visual molecular dynamics, *Journal of molecular graphics*, 14 (1996) 33-38.
- [28] A. Stukowski, Visualization and analysis of atomistic simulation data with OVITO—the Open Visualization Tool, *Modelling and Simulation in Materials Science and Engineering*, 18 (2009) 015012.
- [29] M. Winger, D. Trzesniak, R. Baron, W.F. van Gunsteren, On using a too large integration time step in molecular dynamics simulations of coarse-grained molecular models, *Physical Chemistry Chemical Physics*, 11 (2009) 1934-1941.
- [30] S.J. Marrink, X. Periole, D.P. Tieleman, A.H. de Vries, Comment on “On using a too large integration time step in molecular dynamics simulations of coarse-grained molecular models” by M. Winger, D. Trzesniak, R. Baron and WF van Gunsteren, *Phys. Chem. Chem. Phys.*, 2009, 11, 1934, *Physical Chemistry Chemical Physics*, 12 (2010) 2254-2256.
- [31] R.W. Hockney, J.W. Eastwood, *Computer simulation using particles*, crc Press, 1988.
- [32] J.G. Kirkwood, E.M. Boggs, The radial distribution function in liquids, *The Journal of Chemical Physics*, 10 (1942) 394-402.